Solution Mining Calculations for SPR Caverns*

Anthony J. Russo
Sandia National Laboratories
Albuquerque, New Mexico, USA

ABSTRACT

Several simulation programs have been used in the development of solution mining schedules for the design of SPR caverns. One of these programs, having the code designation SANSMIC, which predicts cavern shape and volume as a function of prescribed flow parameters, was developed to facilitate the calculation of shape changes while leaching is proceeding at the same time that the cavern is being filled with oil (leach-fill) and when oil is being withdrawn by fresh water displacement.

The theory and overall numerical procedures used in SANSMIC are described. Implicit, finite difference methods are used to solve an axisymmetric mass conservation problem. Calculated results are given which exercise each of the code options, and comparisons with other calculations and data from SPR caverns currently being leached are given.

INTRODUCTION

The United States Strategic Petroleum Reserve (SPR) consists of an underground oil storage system that uses caverns leached in salt domes near the Gulf of Mexico and a former salt mine on Weeks Island, Louisiana. Some of the cavern space, formed during commercial brining operations, was available for storage shortly after the program began; however, because this space was less than 250 million barrels, and storage of up to 1 billion barrels is being considered, the Department of Energy (DOE) has undertaken an extensive solution mining program.

The new leached caverns will each hold 10 million barrels of oil. They are approximately 2000 feet tall with the cavern roofs set several thousand feet below the surface. The caverns are designed to accommodate five withdrawal cycles of oil with the oil being displaced by fresh water. Fresh water displacement causes the bottom of the cavern to grow faster than the top. Therefore, initially, the bottom diameter (160 feet) is made smaller than the top diameter (240 feet) so that the shape will not deviate significantly from cylindrical during the cavern lifetime.

Because there was urgency to fill the reserve as rapidly as possible, considerable attention was given to devising a leaching scheme which would yield not only the desired size and shape of cavern but would do it in the shortest practical time. At one time this appeared to be accomplished best by using a leach-fill strategy in which the cavern would be simultaneously filled with oil as the leaching proceeded. To start the cavern, several wells could be drilled and simultaneously leached until the cavities coalesced to form a sump.

The need to model the solution mining process in order to plan and develop these new caverns was obvious. However, because no project of this magnitude had ever been attempted before, confidence in existing models had to be tempered. One of the tools that had been successfully used to develop smaller caverns was the SMRI program SALT77 (Saberian, 1977). This program, or code, proved very useful for planning some portions of the leaching program and developing early leaching schedules. The need to handle moving blanket problems (necessary in leach-fill and oil withdrawal analyses), which SALT77 was not structured to do, and to perform a very large number of calculations efficiently, led to the development of a new program, code SANSMIC. This program utilizes the same dissolution model as SALT77 but includes new diffusion, plume and insolubles models and uses an implicit numerical formulation. This paper describes the models used in SANSMIC and its application to the SPR program.

THEORY

Basic Equations

The details of the theory used in developing the computer program SANSMIC are contained in Russo (1981);

*This work performed at Sandia National Laboratories supported by the U.S. Department of Energy under contract DE-AC04-76-DP00789.

however, for the reader's convenience a brief description of the basic equations and models used will be included here.

When a vertical salt surface is exposed to unsaturated brine, a negatively buoyant dissolution boundary layer is formed next to the surface. Application of a momentum integral analysis to this boundary layer and a series of verification experiments by Durie and Jessen (1964) showed that when the peak fall velocity of this boundary layer was large compared to the edge or bulk velocity of the brine, the dissolution rate at a given temperature varied only with the bulk concentration of the brine and the distance along the boundary layer. Their experiments also showed that the transition to turbulence occurred in very small length scales (typically millimeters). By analogy with turbulent heat transfer by natural convection on a long vertical surface, the distance dependence of the dissolution rate could be neglected (Kreith, 1958, p. 310). The salient results of this dissolution analysis are summarized in Saberian (1977).

The recession rate of a large vertical wall of salt dissolving under the influence of natural convection can be correlated as a function of only the bulk fluid specific gravity, C, at temperatures near 70°F,

$$\frac{dr}{dt} = 45.654996\,C^4 - 232.29310\,C^3 + 469.52470\,C^2 - 470.37554\,C + 232.73686 - 45.203241/C \text{ ft/hr.} \quad (1)$$

The recession rate varies with wall angle, θ, measured from the vertical so that $\theta = 90$ is an upward facing surface and $\theta = -90$ is a downward facing surface, according to

$$\left.\frac{dr}{dt}\right|_{\theta \geq 0} = \left.\frac{dr}{dt}\right|_{\theta=0} [\cos\theta]^{1/2}$$
$$\left.\frac{dr}{dt}\right|_{\theta<0} = \left.\frac{dr}{dt}\right|_{\theta=0} \left\{1 + 0.22\left[1 - \sqrt[3]{\frac{\theta + 45°}{45°}}\right]\right\}. \quad (2)$$

To use these recession rate correlations to calculate cavern formation shapes, the specific gravity of the brine as a function of height must be determined.

If it is assumed that, except for the buoyant plume region above the fresh water injection point and the salt surface boundary layer, the radial concentration gradient is negligible, the theory of stratified enclosures can be used to find C.

An approximate theory has been developed for treating combined natural and forced convection in stably stratified enclosures (Rahm and Walin; 1979, 1981). In this model the natural convection is induced by wall sources weak enough so that the thermal or concentration boundary layer variations are smaller than the total variation due to stratification. The result of this analysis is that the variation of specific gravity with height in the bulk of the fluid is given by Equation (3) for axisymmetric caverns.

$$\frac{\partial C}{\partial t} + \left(\frac{M_o}{A} - \frac{2D}{r}\frac{dr}{dz}\right)\frac{\partial C}{\partial z} + \frac{2DS_d(C - \hat{C})}{r\cos\theta} = D\frac{\partial^2 C}{\partial z^2} \quad (3)$$

where

M_o = the total externally induced volume flow rate
A = the cavern cross sectional area
D = the diffusion coefficient of salt in water
r = the cavern radius
S_d = a source coefficient defining the wall boundary condition by $\partial C/\partial\xi|_{y=0} = S_d(C - \hat{C})$
$\hat{C}$ = the specific gravity of the fluid at the wall ($\xi = 0$). Taken to be the saturation value of 1.202.
t = time

and

θ = the wall angle with respect to vertical.

Equation (3) is a mass conservation equation which balances the rate of salinity increase (first term) with the sum of the net convective flux (second term), the rate of salt dissolution at the walls (third term) and the diffusive flux (last term).

Equation (3) holds outside the plume region above and below the stagnation level (the level at which the buoyant plume grows large enough to interact with the walls). At the stagnation level the value of specific gravity is used as a boundary condition for the solution of Equation (3) along with a zero derivative condition at the upper boundary and a saturation condition at the lower boundary. The stagnation level specific gravity is determined by a mass balance between the injected fluid and dissolved and diffused salt in a control volume. For reverse leaching (injection point above the production point) the control volume is the stagnation level mesh increment, whereas for direct leaching (injection point below the production point) the control volume is the region between the injection and stagnation levels. The stagnation level is estimated from a simple unconstrained buoyant plume model.

Plume Model

Because the mixing within the plume is usually rapid, an analysis of plume dynamics based on the assumption of a uniform specific gravity and velocity within the plume (top hat model) is appropriate. Morton (1956) presents the results of such an analysis as a set of equations which describe the dynamics of an unconstrained steady plume,

$$\frac{d(b^2u)}{dz} = 2\alpha bu$$

$$\frac{d(b^2u^2)}{dz} = 2b^2g(C_o - C)$$

$$\frac{d(b^2ug(C_o - C))}{dz} = 2b^2ug\frac{dC_o}{dz} \qquad (4)$$

where

b = the effective plume radius
C and C_o = fluid specific gravities in and out of the plume
u = the plume velocity in the vertical (z) direction
g = the acceleration of gravity

and

α = is an entrainment coefficient.

When the plume is rising through a stably stratified fluid ($\partial C_o/\partial z < 0$) it will rise to a certain level and stop, and its radius will grow indefinitely. This level is denoted by the plume stagnation level in Figure 1. If the plume is rising in an unstably stratified fluid, it will continue to rise and grow until it interacts with the cavern walls, which then constrain the plume and change its rise rate. The level at which this interaction occurs (the level at which the plume radius equals 0.7 of the cavern radius) will also be denoted as the plume stagnation level, because in either case the entire plume flow is deposited in the fluid cell containing this level.

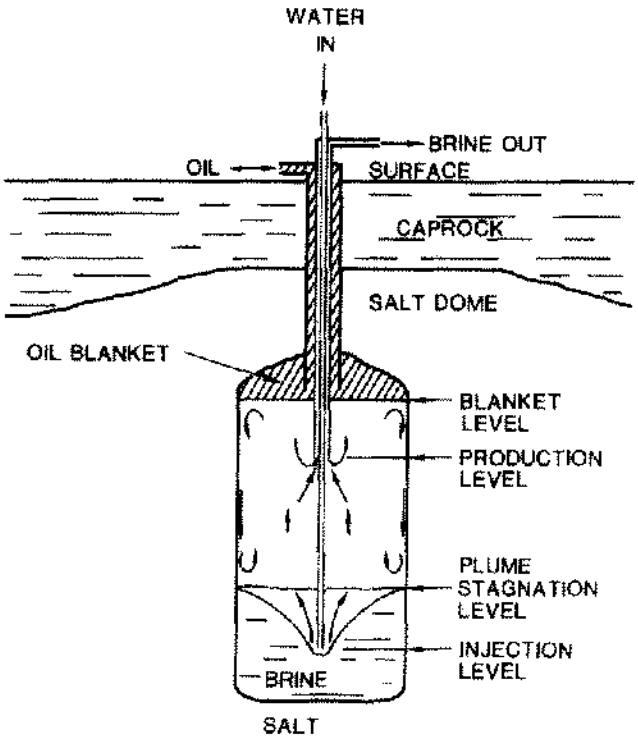

Figure 1. Cavern Geometry and Flow Regions for Direct Leaching

Diffusion Model

The diffusion coefficient, D, which appears in Equation (3), is a strong function of whether the brine is stably or unstably stratified. For stable concentration gradients, D is just the molecular diffusion coefficient, D_{mol}, which is very small (1.4×10^{-5} cm^2/sec). When the concentration gradient is positive, however, (unstable case), a much larger eddy diffusion coefficient, D_e, must be used. An instability analysis given in Russo (1981, p. 9) indicates that an appropriate mixing length, ℓ, to use in calculating D_e when wall effects are ignored is

$$\ell = \left(\frac{6\pi}{\alpha}\right)^{3/4}\left(\frac{2\nu^2 C}{dC/dz\,g}\right)^{1/4} \qquad (5)$$

where

α = the entrainment coefficient
ν = the local kinematic viscosity of the brine
g = the gravitational acceleration.

If it is assumed that the eddy diffusion coefficient is proportional to the product of velocity and mixing length, and the mixing length is taken as the minimum of cavern radius r, and ℓ, as given in (5),

$$D_e = D_o(dC/dz)^{1/2}\,\mathrm{Min}(r^2, \ell^2). \qquad (6)$$

Equation (6) is the final form of the eddy diffusion coefficient to be used in Equation (3) where $D = D_{mol} + D_e$. The value of D_o used was 31.7 ft$^{1/2}$/sec taken from the data of (Knapp, 1979), and the value of α in Equation (5) which best fit a limited amount of data taken from Bryan Mound well 104 was 0.064. This value of α is not far from other experimentally determined values for buoyant plumes that are typically about 0.08 (Morton, 1956, p. 14).

Insolubles Model

Part of the input data required to run SANSMIC is the specification of the volume percent of insolubles in the salt formation. A sample of salt from the dome at Bryan Mound, Texas was analyzed to determine the insoluble particulate size distribution. Most of the insolubles were anhydrite particles between 20 and 400 micrometers average diameter, with a peak at 250 micrometers. Assuming Stokes drag on spherical particles, the settling velocity for each particle size over the range 0 to 400 micrometers was calculated and the integrated fraction that would fall out in an upward velocity field was calculated as a function of fluid velocity. A curve fit to these results, Equation (7), is

included in the code to establish the fraction of insolubles that fill the cavern sump or are discharged,

$$f = 0.5/(1 + 0.00231v) + 0.5e^{-0.002v} \quad (7)$$

where

f = the total fall fraction

and

v = the upward fluid velocity (ft/hr).

The code keeps account of the insolubles that fall and raises the sump floor accordingly as well as increasing the wall recession rate in proportion to the insolubles freed at each level.

Numerical Method

The cavern space to be solution mined is divided into N-equal-sized vertical increments with a mesh point located at each of the N + 1 boundary planes. All values within an increment are assumed to be represented by the value at its lower boundary. The initial radius and concentration for each increment, the oil-brine interface level, injection and production levels, and the injection flow rate are defined for each case.

At every third time step the Equations (4) are solved, using the Sandia system library integration routine ODERT, for the plume concentration, flow rate and stagnation level. At each time step the concentration in the mesh increment containing the stagnation level is updated by a mass balance between the injected fluid, the remaining brine in the increment volume and the salt which diffused and dissolved during one time step. This concentration serves as one of the boundary values for the solution of Equation (3) above and below the stagnation level.

All the terms except the convective one in Equation (3) are implicitly center differenced in conservation form. Upwind differencing is used on the convective term. The difference equations are solved with a tridiagonal algorithm. The diffusion coefficient is a function of concentration gradient and is calculated by

$$D = D_{mol} + D_o\left(\frac{dC}{dz}\right)_+^{1/2} \mathrm{Min}(r^2, \ell^2) \quad (8)$$

where D_{mol} is the molecular diffusion coefficient, $(dC/dz)_+$ is the specific gravity gradient when positive and zero when the specific gravity gradient is negative. The coefficient D_o is an empirically determined eddy diffusion parameter, and the mixing length ℓ is determined from Equation (5) with $\alpha = 0.064$.

After the solution of Equation (3), the new concentrations are used to calculate the wall recession rate from Equations (1) and (2). The cavern radii are updated and the coefficients of Equation (3) reevaluated in preparation for the next time step.

Because the plume Equations (4) and the concentration Equation (3) are tightly coupled and solved sequentially, some numerical oscillation or bouncing of the plume stagnation level can occur. In order to stabilize the plume and limit the errors due to this oscillation, the stagnation level has been restricted to lie within two mesh intervals below the level previously calculated (it can fall by only two spaces at a time). Because the time required for the plume to find a stable level is small compared to the leaching time, this approximation should introduce little error.

The solution to any differential equation is determined by its boundary conditions. The boundary condition at the stagnation level is computed at each time step from the values at the previous time step and errors tend to accumulate. The cavern volume and shape are very sensitive to the boundary values used, so it is important to limit the errors on these values. This is accomplished by performing a global mass balance at each time step and computing a correction factor for the concentrations and boundary conditions to be used in the next time step. This forces the mass concentration in the time integration to follow a self-consistent and self-correcting path.

The total mass of brine in the cavern, M_T, is computed by the time integral

$$M_T = m_{co} + \int_0^T \left(\sum_1^N \frac{VSR}{\Delta t} C_{salt} + Q_i C_i - (Q_o + Q_{fill})C_p\right) dt \quad (9)$$

where

Q_o = the outlet volume flow rate for no oil flow
Q_{fill} = the oil volume flow rate
C_p = the brine S.G. at the production level
T = the time period
VSR = the volume of salt removed from the increment Δz in the time increment Δt
m_{co} = the initial mass of brine in the cavern

and

N = the number of mesh intervals used.

The total mass of brine in the cavern, M_c, is computed by

$$M_c = \sum_{I=1}^{N} \pi r^2(I)\,\Delta z\, C(I). \quad (10)$$

The correction factor for the stagnation level boundary condition is then found by

$$\text{Corr. Fac} = \frac{M_T}{M_c}. \quad (11)$$

This factor is always close to 1 and is printed out with each result. A value of 1 for the correction factor only means, of course, that the calculation is self-consistent, and not that it is modeling any physical situation correctly.

Dissolution Rate Correction

When the previously described models and numerical method are compared to field data, it is found that for cases in which reverse leaching is employed, with the injection point well below the protective roof oil blanket, the dissolution rate is larger than predicted by Equation (1). It is believed that this occurs because, as is noted at the beginning of the Theory section, the dissolution correlations are only valid when the bulk fluid flow velocities are much less than the peak boundary layer velocity. For the case described above, the plume rising near the center of the cavern and the return flow along the periphery generate a toroidal vortex, the velocity of which may be much greater than that calculated for plain plug flow.

An accurate model of the vortical velocity field, which is a function of raw water injection rate, pipe string settings and cavern geometry, has not yet been included in the code. Instead, a model based on heuristic arguments and some empirical fits has been used to calculate a dissolution rate correction term, E_{diss}. For the region between the injection height, Zi, and the oil blanket height, Zb,

$$E_{diss} = 0.0067\ \mathrm{MIN}(L\Delta z/200,\ 2,\ R/25)\sqrt{Q_i}\ [(1 - L_v)L_r]^{0.25}$$

and below Zi

$$E_{diss} = E_{diss\,Zi}\, e^{-2.5L_r}$$

where

L_r = L_v/L
L = $(Zb - Zi)\ 1.15/\Delta z$
L_v = $L - (Z - Zi)/\Delta z$
Δz = length of a vertical mesh increment,

and

R = cavern radius at the injection level.

RESULTS

Comparison with SALT77

The SMRI code has been verified for the cases of bottom injection and brine removal at the top (direct leaching) and top injection and bottom brine removal (reverse leaching) (Saberian, 1977). Since a degree of confidence has been established for the SMRI code for the simple direct and reverse leaching cases, the first comparison to be made will be for leaching a 0.625-foot-radius borehole in the direct mode for 40 days at a flow rate of 10603.5 ft^3/hour (1322 gallons/minute) of water with a S.G. of 1.0108, and then in the reverse mode at the same flow rate for 100 days. Figure 2 shows a comparison of the cavern shapes calculated with the SMRI code and the new code. The cavern shapes are almost identical, differing only near the injection region by about 10%. The overall cavern volumes differed by 5.5% at the end of the mining process. The produced brine saturation percent differed by less than 0.3%.

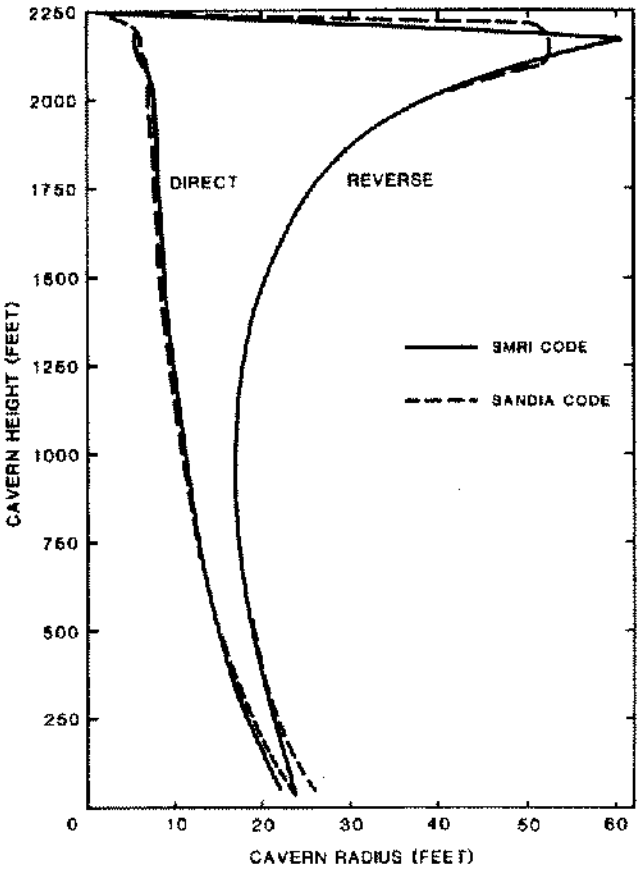

Figure 2. A Comparison of Calculated Cavern Shapes

Bryan Mound Cavern 106

Some data are available from the direct leaching of Bryan Mound Cavern 106. Two wells, A and B, were simultaneously leached for one day at a flow rate of 1507 ft^3/hr, then for 84 days at an average flow rate of 6596 ft^3/hr. The injection water was assumed to have a specific gravity of 1.0108. A 7-inch injection tubing was set at a depth of 4450 feet and a 10¾-inch production casing was set at a depth of 2280 feet. The initial borehole size was taken to be 15 inches in diameter. In actuality, the two wells would eventually coalesce with each other and with a third well started later, thereby forming Cavern 106. All simulations and data discussed here are for the period when each well forms a separate cavity. This case was simulated with both the SMRI code and the new code neglecting insolubles. The results are shown in Figure 3 along with sonar caliper data recorded by the Dowell Corporation between July 2 and July 6, 1980. The radii data plotted in Figure 3 are effective radii, which, if the cavern cross section were circular, give the same area as that measured (the same as the RMS radius). The calculated curves practically fall on each other, differing by 2% or less over the whole depth, but both un-

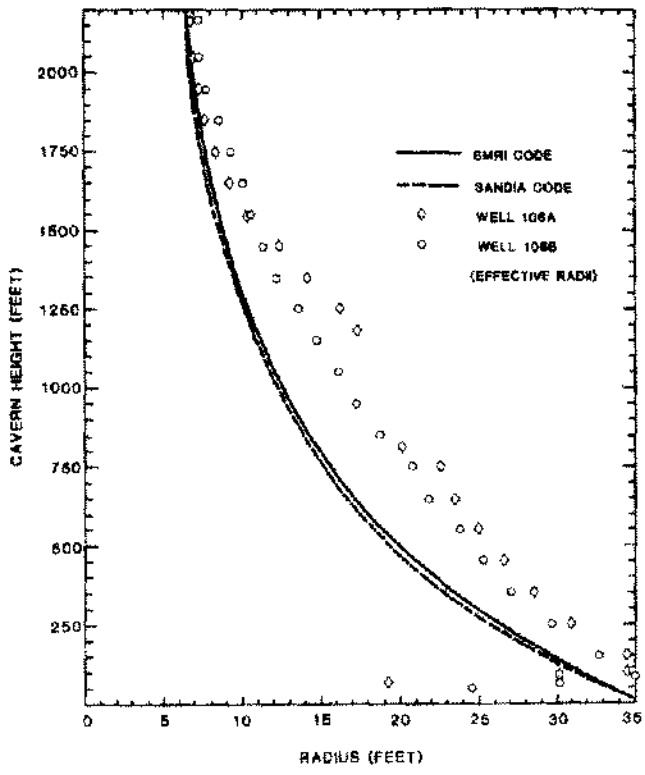

Figure 3. A Comparison of Calculated and Measured Cavern Shapes for Bryan Mound Cavern 106

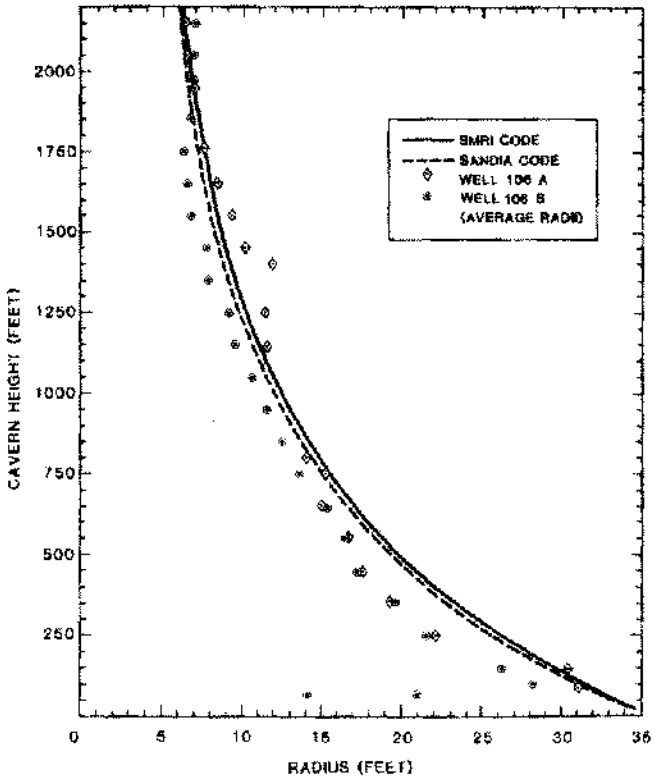

Figure 4. A Comparison of Calculated and Measured Shapes for Bryan Mound Cavern 106

derestimate the measured volume by about 20%. This discrepancy could be caused by a number of factors. First, the accuracy of the flow measurements is not known. Error estimates of 20% have been made for some measurements. The assumed temperature for all calculations was 75°F, but the exit temperature of the brine was as high as 98°F during some of the leaching. The insolubles content was neglected (about 7%). The calculations assume an axisymmetric geometry, but the actual cross sections were not circular. This fact can be significant because the larger surface to volume ratios would cause more salt to dissolve than was estimated. The sonar data was taken in eight directions (5% accuracy is typical for radius sonar data), and if the average value of the radii are taken rather than the RMS value, the results are quite different, indicating a large deviation from circularity. Figure 4 shows the average radius data plotted with the calculated values. This plot indicates a better fit and the calculations even seem to overestimate the cavern size slightly. The asymmetries in the dissolution of the cavern can be caused by the presence of highly soluble sylvite deposits, uneven distribution of anhydrite or other insolubles, or uneven convective mixing of the injected water, none of which can be accounted for in an axisymmetric calculation. Considering all the assumptions that were made, the calculated results seem as good as can be expected.

Comparison with Field Data

Data from two caverns at West Hackberry, Louisiana, which were leached in the direct mode are shown in Figures 5 and 6. Figure 5 shows calculated and measured cavern effective radii after 147 days of leaching with the injection level at a depth of 5000 feet. The calculated and measured volume agree to within 3%, but the calculated radii near the bottom are larger than the sonar measurements by up to 16% near the bottom of the cavern. The average measured flow rate of 123,880 barrels/day is probably fairly accurate, since the volumes agree so well. Because the injection point was, at the end of the flow, buried several hundred feet below the insolubles level, there were a great deal of entrained insolubles suspended in the lower cavern region, which may have reduced the dissolution rate in that region. If that is not the cause of this discrepancy, further modifications to the plume mixing model should be considered.

A similar comparison for cavern WH104 after 156 days of leaching with an average measured flow rate of 138,484 barrels/day is shown in Figure 6. The calculated volume is 12% greater than the measured volume, which indicates that the flow measurements are probably high. The same pattern of overpredicting the cavern radii at the lower end, in this case by 20%, is apparent in Figure 6. For smaller

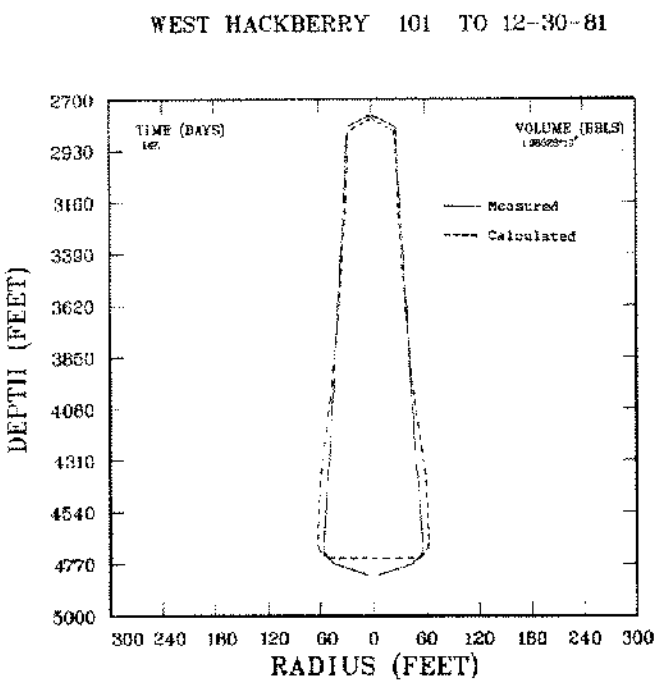

Figure 5. A Comparison of Calculated and Measured Cavern Shapes after Direct Leaching of WH101

diameter caverns where the insolubles depth is not so large, this overprediction has not been observed.

After the sump chimney phase of cavern development is finished, the injection level is usually raised to several hundred feet below the cavern roof and the first phase of reverse leaching is begun. A comparison of calculated and measured cavern shape for cavern WH101 at the end of this phase (189 days) is shown in Figure 7. The calculated and measured volumes are within 2% of each other, but the maximum radii differ by 9%. The calculation near the top of the cavern is strongly influenced by the dissolution rate correction model described in the theory section, and because this is a rough approximation, such deviations can be expected.

Figure 8 shows the same kind of comparison for cavern WH104. In this case, the volumes differ by 4% and the calculated maximum radius is a 10% overestimate. The injection level was set 200 feet below the oil blanket level in this case.

The injection level for the corresponding stage in Bryan Mound Cavern 106 was set 630 feet below the oil blanket and the comparison between measured and calculated cavern shape is shown in Figure 9. The total measured cavern volume is only 1% less than the calculated value. Near the bottom of the upper bulb, the radii differ by about 20% for the same reasons mentioned previously. In addition to errors in the dissolution rate model, it should be remembered that the cavern radii shown are effective values, and that in some cases, including BM106, the ac-

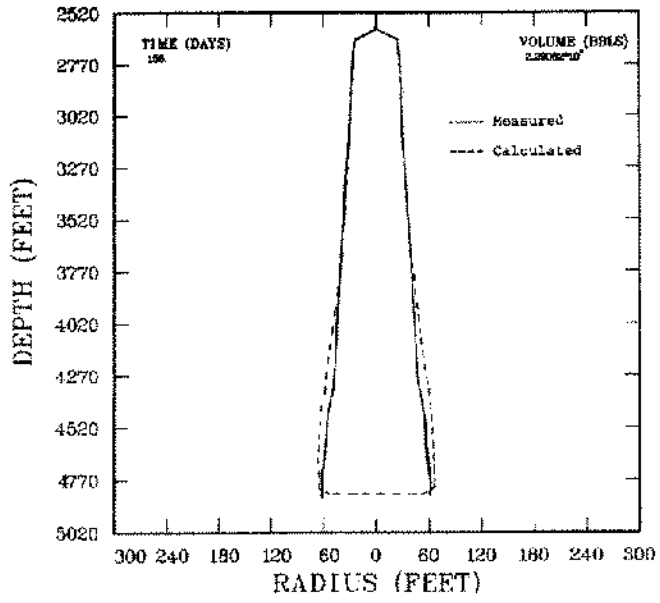

Figure 6. A Comparison of Measured and Calculated Cavern Shapes after Direct Leaching of WH104

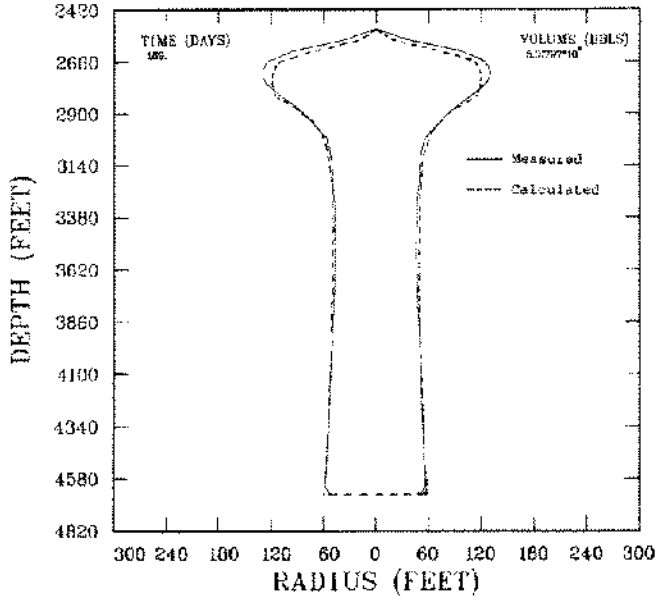

Figure 7. A Comparison of Calculated and Measured Cavern Shapes after Reverse Leaching of WH101

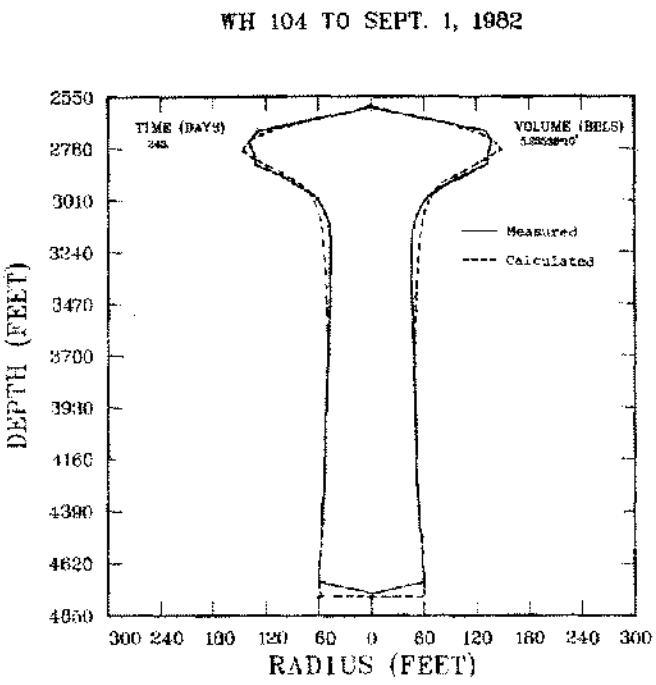

Figure 8. A Comparison of Calculated and Measured Cavern Shapes after Reverse Leaching of WH104

tual cross section deviates markedly from circularity so that the axisymmetric approximation is poor. In all cases, the actual vertical distribution of insolubles was represented by a single number. The estimated error in the measured flow rates used in the calculations was ±10%.

An example of the use of the code to predict cavern growth during oil withdrawal is shown in Figure 10. West Hackberry Cavern 11 is one of the SPR phase one caverns (a cavern produced during commercial brining) which has been filled with oil. The predicted change in cavern shape and volume as the oil is withdrawn by displacement with fresh water and refilled for 5 complete cycles is indicated in this figure. The lower portion of the cavern which is exposed for the longest time, since the oil blanket rises during withdrawal, enlarges at the fastest rate. This type of withdrawal prediction has been made for each cavern to investigate the possibility of cavern coalescence and to evaluate dome subsidence.

CONCLUSIONS

The solution mining code SANSMIC has been developed for calculating the formation of storage caverns in salt. It is applicable to axisymmetric caverns having a single injection and production level. The code uses a vertically stratified mass balance model to calculate the bulk brine salinity which is coupled with an unconfined plume model and an empirical dissolution model to determine the wall re-

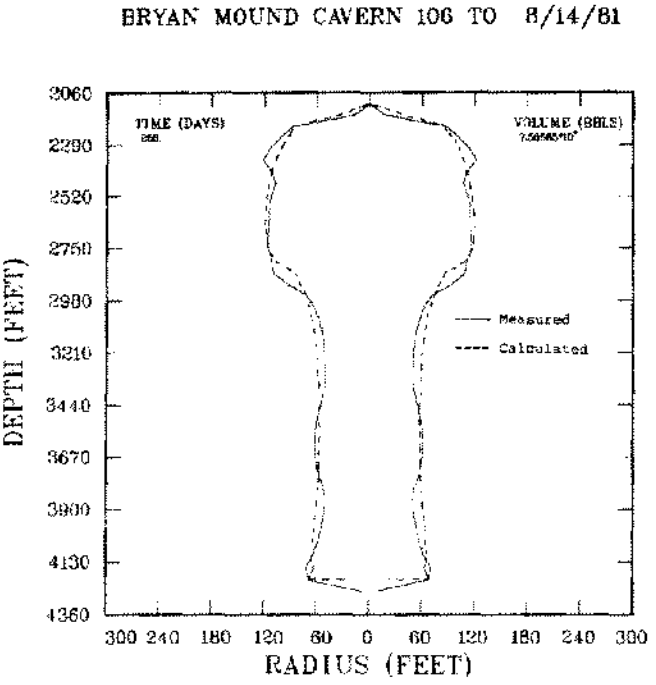

Figure 9. A Comparison of Calculated and Measured Cavern Shapes after Reverse Leaching of BM106

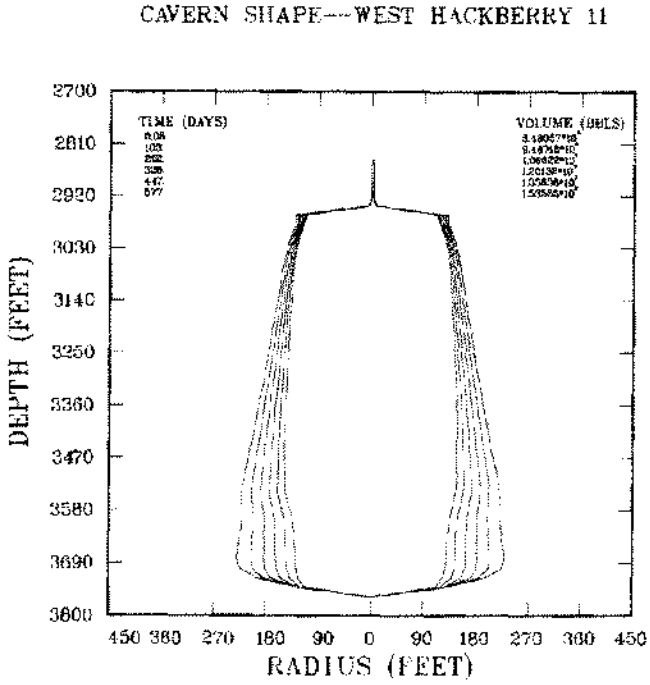

Figure 10. An Example of Calculated Cavern Enlargement for Five Oil Withdrawal Cycles

cession rate. SANSMIC has options for leaching with or without motion of the oil blanket so that leach-fill or oil withdrawal operations can be simulated. The raw water injection options include direct, reverse and zero flow conditions. If knowledge of the local insolubles content or relative salt dissolution rate is available, it can be incorporated into the calculations. The code is currently operational on the Sandia CDC6600/7600 system, the CRAY and VAX11/780 computers.

Comparison of the code results with the SMRI solution mining code SALT77 show good agreement for small caverns in which the injection point is near the top of the cavern and the brine production is at the bottom, or vice versa. The simulation of the development of large SPR caverns has been fairly successful. Almost all of the volume comparisons are within 5% despite raw water temperature fluctuations, cavern asymmetries, and uncertainties in the flow measurements and insolubles distribution. Local deviations in radius of up to 20% have been seen in several caverns, however. It appears that improvements in the flow and dissolution models as well as tighter control of the input variables will be necessary to improve the predictive accuracy of the code.

REFERENCES

Durie, R. N. and F. W. Jessen. 1964. Mechanism of the dissolution of salt in the formation of underground salt cavities; SPE Journal, pp. 183, 190.

Durie, R. N. and F. W. Jessen. 1964. The influence of surface features in the salt dissolution process; SPE Journal, pp. 275, 281.

Knapp, R. M. and A. L. Podio. 1979. Investigation of salt transport in vertical boreholes and brine invasion into fresh water aquifers; ONWI-77, pp. 1, 72.

Kreith, F. 1958. Principles of heat transfer, International Textbook Co. Scranton, p. 310.

Morton, B. R. et al. 1956. Turbulent gravitational convection from maintained and instantaneous sources; Proc. of the Royal Society, Series A, Vol. 234, No. 1196, Jan. 24, pp. 1, 23.

Rahm, L. and G. Walin. 1979. On thermal convection in stratified fluids; Geophys. Astrophys. Fluid Dynamics, v. 13, pp. 51, 65.

Rahm, L. and G. Walin. 1979. Theory and experiment on the control of the stratification in almost enclosed containers; J. Fluid Mech. 90, pp. 315, 325.

Russo, A. J. 1981. A solution mining code for studying axisymmetric salt cavern formation; Sandia Report SAND81-1231, pp. 1, 32.

Saberian, A. and A. L. Podio. 1977. A computer model for describing the development of solution-mined cavities, IN SITU, 1(1), pp. 1-36.

Walin, G. 1971. Contained non-homogeneous flow under gravity or how to stratify a fluid in the laboratory; J. Fluid Mech. 48, pp. 647, 672.